

1 **Measurement report: Brown Carbon Aerosol in Polluted Urban Air of North China Plain:**  
2 **Day-night Differences in the Chromophores and Optical Properties**

3 **Yuquan Gong<sup>1,2</sup>, Ru-Jin Huang<sup>1,2,3</sup>, Lu Yang<sup>1,2</sup>, Ting Wang<sup>1</sup>, Wei Yuan<sup>1,2</sup>, Wei Xu<sup>1</sup>,**  
4 **Wenjuan Cao<sup>1</sup>, Yang Wang<sup>4,5</sup>, Yongjie Li<sup>6</sup>**

5 <sup>1</sup>State Key Laboratory of Loess and Quaternary Geology, CAS Center for Excellence in  
6 Quaternary Science and Global Change, Institute of Earth Environment, Chinese Academy of  
7 Sciences, 710061 Xi'an, China

8 <sup>2</sup>University of Chinese Academy of Sciences, Beijing 100049, China

9 <sup>3</sup>Institute of Global Environmental Change, Xi'an Jiaotong University, Xi'an 710049, China

10 <sup>4</sup>School of Geographical Sciences, Hebei Normal University, Shijiazhuang, China

11 <sup>5</sup>State Key Joint Laboratory of Environmental Simulation and Pollution Control, Beijing, China

12 <sup>6</sup>Department of Civil and Environmental Engineering, Faculty of Science and Technology,  
13 University of Macau, Taipa, Macau SAR 999078, China

14 Correspondence: E-mail: [rujin.huang@ieecas.cn](mailto:rujin.huang@ieecas.cn) (R.-J.H)

15 **Abstract.** Brown carbon (BrC) aerosol is light-absorbing organic carbon that affects radiative  
16 forcing and atmospheric photochemistry. The BrC chromophoric composition and its linkage  
17 to optical properties at the molecular level, however, are still not well characterized. In this  
18 study, we investigate the day-night differences in the chromophoric composition (38 species)  
19 and optical properties of water-soluble and water-insoluble BrC fractions (WS-BrC and WIS-  
20 BrC) in aerosol samples collected in Shijiazhuang, one of the most polluted cities in China. We  
21 found that the light absorption contribution of WS-BrC to total BrC at 365 nm was higher during  
22 the day ( $62 \pm 8\%$ ) than during the night ( $47 \pm 26\%$ ), which is in line with the difference in  
23 chromophoric polarity between daytime (more polar nitrated aromatics) and nighttime (more  
24 less-polar polycyclic aromatic hydrocarbons, PAHs). The high polarity and water solubility of  
25 BrC in daytime suggests the enhanced contribution of secondary formation to BrC during the  
26 day. There was a decrease of the mass absorption efficiency of BrC from nighttime to daytime  
27 ( $2.88 \pm 0.24$  vs.  $2.58 \pm 0.14$  for WS-BrC and  $1.43 \pm 0.83$  vs.  $1.02 \pm 0.49$   $\text{m}^2 \text{g}^{-1} \text{C}^{-1}$  for WIS-BrC,  
28 respectively). Large polycyclic aromatic hydrocarbons (PAHs) with 4–6-rings PAHs and  
29 nitrophenols contributed to 76.7% of the total light absorption between 300–420 nm at night  
30 time, while nitrocatechols and 2–3-ring oxygenated PAHs accounted for 52.6% of the total light  
31 absorption at day. The total mass concentrations of the identified chromophores showed larger  
32 day-night difference during the low-pollution period (day-to-night ratio of 4.3) than during the  
33 high-pollution period (day-to-night ratio of 1.8). The large day-night difference in BrC  
34 composition and absorption, therefore, should be considered when estimating the sources,  
35 atmospheric processes and impacts of BrC.

## 36 **1 Introduction**

37 Light-absorbing organic carbon aerosols, also termed brown carbon (BrC) aerosol, are  
38 ubiquitous in the atmosphere (Iinuma et al., 2010; Yuan et al., 2016; Huang et al., 2021).  
39 Growing evidence has shown that BrC can reduce atmospheric visibility, affect atmospheric  
40 photochemistry, and change regional and global radiation balance (Kirchstetter et al., 2004;  
41 Laskin et al., 2015; Hammer et al., 2016). Besides, some components in BrC, such as polycyclic  
42 aromatic hydrocarbons (PAHs) are highly toxic and carcinogenic, which can adversely impact  
43 human health (Alcanzare, 2006; Zhang et al., 2009; Huang et al., 2014). The extent of these  
44 effects is closely related to the optical properties and chemical composition of BrC, which are  
45 still not well understood.

46 BrC is often classified into water-soluble (WS-BrC) and water-insoluble (WIS-BrC)  
47 fractions because these two fractions are largely different in chemical composition and light  
48 absorption. For example, abundant nitrophenols were detected in WS-BrC, while polycyclic  
49 aromatic hydrocarbons (PAHs) were the main component of WIS-BrC (Huang et al., 2018;  
50 Huang et al., 2020). The difference in BrC chemical composition is associated with the emission  
51 sources. For example, methyl nitrocatechols are specific to biomass burning, while PAHs are  
52 mainly emitted by fossil fuel combustion (Kitanovski et al., 2012; Dat and Chang, 2017).  
53 Atmospheric oxidation can further complicate the BrC chromophores dynamically, leading to  
54 light-absorbing enhancement or bleaching. For example, Li et al. (2020) reported that the mass  
55 absorption efficient (MAE) of some nitroaromatic compounds (e.g., nitrocatechols) from the  
56 biomass burning can enhance about 2–3 times by oxidation to generate secondary  
57 chromophores. Yet, prolonged photo-oxidation reactions (exposure to sunlight for few hours)  
58 of these nitroaromatic can generate small fragment molecules (e.g., malonic acid, glyoxylic  
59 acid) and rapidly reduce the particle absorption (Hems and Abbatt, 2018; Wang et al., 2019b;  
60 Li et al., 2020). The complexity in composition and sources, as well as the dynamics in their  
61 atmospheric processing limit our understanding in BrC chromophores and their links to light  
62 absorption.

63 In recent years, a growing number of studies have investigated the chromophore  
64 composition of BrC and found that nitro-phenols, low ring acids/alcohols, PAHs and carbonyl

65 oxygenated PAHs (OPAHs) were the major chromophores in BrC (Teich et al., 2017; Yuan et  
66 al., 2020; Huang et al., 2020). Some chromophores in BrC can be generated from both primary  
67 emission and secondary formation. For example, 4-nitrophenol and 4-nitrocatechol can be  
68 emitted directly from biomass burning and can also be generated through photo-oxidation  
69 reactions (Kitanovski et al., 2012; Yuan et al., 2020). The differences in emission sources or  
70 atmospheric oxidation conditions have a significant effect on the chemical composition of BrC  
71 chromophores. Previous studies mainly focused on seasonal variations of BrC chromophores  
72 (Wang et al., 2018; Kasthuriarachchi et al., 2020; Yuan et al., 2021), and the diurnal variation  
73 of WS-BrC in fluorescence and inorganic fractions (Deng et al., 2022; Zhan et al., 2022),  
74 however, the research of BrC chemical composition on day-night differences is scarce. In this  
75 study, the optical properties and chemical composition of the WS-BrC and WIS-BrC in daytime  
76 and nighttime were measured with a high-performance liquid chromatography–photodiode  
77 array–high-resolution mass spectrometry platform (HPLC-PDA-HRMS) in PM<sub>2.5</sub> samples  
78 collected in Shijiazhuang, one of the most polluted cities in the Beijing-Tianjin-Hebei region.  
79 Besides, the relationship between the concentration and light-absorbing contributions of the  
80 BrC subgroups was analyzed. The object of this study is to investigate the day-night differences  
81 in the optical properties and chromophore composition of BrC and to explore the effect of  
82 primary emissions and atmospheric processes on the light absorption and chemical composition  
83 of BrC.

## 84 **2 Experimental**

### 85 **2.1 Sample collection.**

86 Day and night PM<sub>2.5</sub> samples were collected on the quartz-fiber filters (8\*10 in., Whatman,  
87 QM-A; filters prebaked at 750 °C, over 3 h) through a high-volume air sampler (Hi-Vol PM<sub>2.5</sub>  
88 sampler, Tisch, the velocity of flow ~1.03 m<sup>3</sup> min<sup>-1</sup>, Cleveland, OH) from 17 January to 13  
89 February 2014. Daytime samples were collected from 08:30 to 18:30 (~10 hours), and nighttime  
90 samples are collected from 18:30 to the next day at 8:30 (~14 hours). After collection, the  
91 samples were stored in a freezer (-20°C) until analysis. The sampling site was located on the  
92 rooftop of a building (~15 m above ground) in the Institute of Genetics and Developmental

93 Biology, Chinese Academy of Sciences (38.2° N, 114.3° E), which is surrounded by a  
94 residential–business mixed zone.

## 95 **2.2 Light Absorption Measurement.**

96 A portion filter (about 0.526 cm<sup>2</sup> punch) was taken from collected samples and sonicated  
97 for 30 min in 10 mL of ultrapure water (>18.2 MΩ) or methanol (J. T. Baker, HPLC grade), and  
98 then the extracts WS-BrC and methanol soluble BrC (MS-BrC) were obtained. The extracts  
99 were filtered with a 0.45 μm PVDF (water soluble) or PTFE (water insoluble) pore syringe  
100 filter to remove insoluble substances. The light absorption spectra of the filtrate were tested  
101 using a UV-VIS spectrophotometer (Ocean Optics) over the range from 250 nm to 700 nm,  
102 equipped with a liquid waveguide capillary cell (LWCC-3100, World Precision Instruments,  
103 Sarasota, FL, USA), following the method of Hecobian et al. (2010). To ensure reliable  
104 absorbance measurements (Absorbance between 0.2 to 0.8 at 300 nm in this study), the filtrate  
105 was diluted with appropriate folds before absorption spectra measurements. In this study, the  
106 light-absorbing of WIS-BrC is obtained by MS-BrC minus WS-BrC. As shown in Figure S1,  
107 the summed absorbance of WS-BrC and WIS-BrC is very close to the absorbance of MS-BrC  
108 (difference less than 5%). Therefore, the interferences of solvent and pH on the measurement  
109 of WIS-BrC should be very limited. The pH of the water extracts was not adjusted because  
110 highly diluted water extracts was used to measure the light absorption, and little change of pH  
111 was observed for water extracts of different samples. The light absorption coefficient (Abs) and  
112 absorption data were calculated following the equation:

$$113 \quad Abs_{\lambda} = (A_{\lambda} - A_{700}) \frac{V_l}{V_b \times l} \times \ln(10)$$

114 where  $Abs_{\lambda}$  (Mm<sup>-1</sup>) represents the sample absorption coefficient at wavelength of  $\lambda$ ;  $A_{\lambda}$  is the  
115 absorbance recorded (Random wavelength);  $A_{700}$  for explaining baseline drift as the reference  
116 during data analysis. To account for baseline drift that may occur during analysis, absorption at  
117 all wavelengths below 700 nm are referenced to that at 700 nm where there is no absorption for  
118 BrC extracts.  $V_l$  (ml) is the total volume of solvent (water or methanol) used to extract the  
119 quartz-fiber filters;  $V_b$  (m<sup>3</sup>) represents the volume of through the filter sample of the air;  $l$  (0.94  
120 m) is the optical path length of UV-VIS spectrophotometer and  $\ln(10)$  is the absorption  
121 coefficient with base-e, which is the natural logarithm by using the logarithm conversion with

122 the base-10.

123 About the mass absorption efficiency (MAE) of the filter extracts at wavelength of  $\lambda$  can be  
124 defined as:

$$125 \quad MAE_{\lambda} = Abs_{\lambda}/C_{OM}$$

126 where  $C_{OM}$  ( $\mu\text{g m}^{-3}$ ) stands for the concentration of water-soluble organic carbon (WSOC) or  
127 methanol extracts methanol-soluble organic carbon (MSOC). The concentrations of WSOC  
128 were measured with a TOC-TN analyzer (TOC-L, Shimadzu, Japan). The concentration of OC  
129 was measured by a thermal-optical carbon analyzer (DRI, Model 2001) with the IMPROVE A  
130 protocol (Chow et al., 2011). Note that MSOC is usually replaced with OC because previous  
131 studies have shown that methanol has a high extraction efficiency (~90%) for OC. But it is  
132 difficult to completely extract the OC by methanol (Chen and Bond, 2010; Cheng et al., 2016;  
133 Xie et al., 2019). Here, WISOC is obtained by MSOC minus WSOC.

134 The wavelength dependence that the light absorption chromophore of solution can be  
135 characterized by this equation:

$$136 \quad Abs_{\lambda} = K \cdot \lambda^{-AAE}$$

137 where K is the fitting parameter of the extracts which is constant related to the chromophoric  
138 concentration; AAE is known as the absorption Ångström exponent, which depends on the  
139 types of chromophores in the solution. In this study, AAE was calculated by linear regression  
140 of  $\log_{10} Abs_{\lambda}$  versus  $\log_{10} \lambda$  at 300–400 nm.

141 The MAE of standards samples ( $MAE_{S,\lambda}$ ), e.g., 4-nitrocatechol and 4-nitrophenol, in the  
142 water or methanol solvent at a wavelength of  $\lambda$  were calculated as the Laskin et al. (2015)

$$143 \quad MAE_{S,\lambda} = \frac{A_{\lambda} - A_{700}}{l \times C} \ln(10)$$

144 where C ( $\mu\text{g mL}^{-1}$ ) is the concentration of the standards in the extracts.

### 145 **2.3 BrC Chemical composition analysis.**

146 The main chromophores in WS-BrC and WIS-BrC were identified by the HPLC-PDA-  
147 HRMS platform (Thermo Electron, Inc.), and the details are presented in our previous study  
148 (Huang et al., 2020). Firstly, the filter samples ( $3.5\sim 48.3 \text{ cm}^2$ ) were ultrasonically extracted  
149 with 6 mL of the ultrapure water for 30 min and repeated two times. The extracts were filtered  
150 through a PVDF filter ( $0.45 \mu\text{m}$ ) to remove insoluble materials. Then the solution was subjected

151 to an SPE cartridge (Oasis HLB, USA) to remove water-soluble inorganic salt ions. On the  
152 other hand, the residual filters were dried and the WIS-BrC fractions were further extracted two  
153 times with 6 mL of methanol for 30 min. to extract the WIS-BrC fractions. Afterward, the  
154 extracts of WS-BrC and WIS-BrC chromophores were dried with a gentle stream of nitrogen  
155 and then redissolved in 150  $\mu$ l of ultrapure water and methanol.

156 The BrC factions were analyzed by an HPLC-PDA-HRMS platform (including the Dionex  
157 UltiMate system and the high-resolution Q Exactive Plus hybrid quadrupole-Orbitrap mass  
158 spectrometer). Here, the extracts were loaded onto a Thermo Accucore RP-MS column by the  
159 binary solvent with an aqueous solution containing 0.1% formic acid and methanol solution  
160 containing 0.1% formic acid as mobile phases L<sub>1</sub> and L<sub>2</sub>, eluting at a flow rate of 0.3 mL min<sup>-1</sup>.  
161 The process of gradient elution here was set as follows: firstly, aggrandize linearly the  
162 concentration of L<sub>2</sub> from 15% to 30% in the preliminary 15 minutes, and then linearly increased  
163 to 90% from 15 to 45minutes, held at 90% from 45 to 50 minutes, afterward decreased to 15%  
164 from 50 to 52 minutes and held there for 60 minutes. The Q Exactive Plus hybrid quadrupole-  
165 Orbitrap mass spectrometer, negative/positive mode ESI (-)/ESI (+) for details usage and data  
166 processing can refer to in the article by Huang et al. (2020) and Liu et al. (2016). Briefly,  
167 HPLC/PDA/HRMS platform was employed in ESI (-) and ESI (+) mode to acquire BrC  
168 fractions that mass range from m/z 100 to 800. Strongly polar aromatic hydrocarbons like  
169 nitrophenol and carboxylic acid are preferentially ionized in ESI (-) mode (Lin et al., 2017).  
170 OPAHs and nitrogen heterocyclic PAHs were quantified in ESI (+) mode, while PAHs were  
171 detected by PDA spectroscopic analysis due to their super low ionization efficiency in ESI. The  
172 absorption spectra of chromophores were measured by a PDA detector in the wavelength range  
173 of 190-700 nm. The results of this study were corrected by a blank.

174 The elemental composition of individual chromatographic peaks was assigned with the  
175 molecular formula calculator in Xcalibur 4.0 software using a mass tolerance of  $\pm 3$  ppm and  
176 the maximum numbers of atoms for the formula calculator were set as 30 <sup>12</sup>C, 60 <sup>1</sup>H, 15 <sup>16</sup>O, 3  
177 <sup>14</sup>N, 1 <sup>32</sup>S, 1 <sup>23</sup>Na. To eliminate the chemically unreasonable formulas, the identified formulas  
178 were constrained by setting  $0.3 \leq H/C \leq 3.0$ ,  $0.0 \leq O/C \leq 3.0$ ,  $0.0 \leq N/C \leq 0.5$ ,  $0.0 \leq S/C \leq 0.2$   
179 in ESI- mode and  $0.3 \leq H/C \leq 3.0$ ,  $0.0 \leq O/C \leq 3.0$ ,  $0.0 \leq N/C \leq 1.3$ ,  $0.0 \leq S/C \leq 0.8$  in ESI+

180 mode, as suggested in a previous study (Lin et al., 2012). Further, the calculated neutral  
181 molecular formulas that did not fit the nitrogen rule were excluded. In total, 20 WS-BrC  
182 chromophores (two quinolines, four 2-3 ring OPAHs, four nitrocatechols, six nitrophenols and  
183 four aromatic alcohols & acids) and 18 WIS-BrC chromophores (three 4-ring OPAHs and 15  
184 PAHs) were identified and their concentrations were quantified with authentic standards (28  
185 species) or surrogates (10 species) (see Table S1). Thereinto, the WS-BrC chromophores,  
186 benzanthrone (21#) and benzo[b]fluoren-11-one (22#) were quantified by mass spectrometry  
187 analysis in either negative or positive ESI mode, while the rest of WIS-BrC chromophores were  
188 quantified by PDA spectroscopic analysis due to their super low ionization efficiency in ESI  
189 (see Table S1).

### 190 **3 Results and discussion**

#### 191 **3.1 Optical properties of BrC during the day and night.**

192 Figure 1 (a) shows the average absorption spectra of WS-BrC and WIS-BrC at the  
193 wavelength range between 300 and 500 nm during the day and the night. It can be seen that the  
194 light absorption of both WS-BrC and WIS-BrC sharply increased toward the short wavelength.  
195 The average absorbance of WS-BrC is  $46.04 \pm 35.92 \text{ Mm}^{-1}$  (at 365 nm) during the day that is  
196 higher than the night ( $35.68 \pm 35.50 \text{ Mm}^{-1}$ ). However, the light absorption of WIS-BrC at 365  
197 nm is much lower during the night ( $27.90 \pm 24.80 \text{ Mm}^{-1}$ ) than during the day ( $40.89 \pm 23.42$   
198  $\text{Mm}^{-1}$ ). The day-night differences of light absorption of WS-BrC and WIS-BrC indicates the  
199 difference in water solubility and polarity of the chromophores. The average AAE of WS-BrC  
200 ( $\text{AAE}_{\text{WS-BrC}}$ ) and WIS-BrC ( $\text{AAE}_{\text{WIS-BrC}}$ ) during the day are  $5.10 \pm 0.28$  and  $6.36 \pm 0.45$ ,  
201 respectively, which are lower than those of the night ( $5.51 \pm 0.40$  and  $6.97 \pm 0.80$ , respectively).  
202 Note that both during the day and night the  $\text{AAE}_{\text{WS-BrC}}$  is lower than  $\text{AAE}_{\text{WIS-BrC}}$ , which is  
203 different from findings in previous studies (see Table S2). For example, Huang et al. (2020)  
204 found that the  $\text{AAE}_{\text{WS-BrC}}$  was higher ( $8.2 \pm 1.0$  and  $8.2 \pm 1.0$  in Beijing and Xi'an, respectively)  
205 than that of  $\text{AAE}_{\text{WIS-BrC}}$  ( $5.7 \pm 0.2$  and  $5.4 \pm 0.2$  in Beijing and Xi'an, respectively). Besides,  
206  $\text{MAE}_{365}$  of WS-BrC are 2.0- and 2.5-fold of WIS-BrC during the day ( $2.88 \pm 0.24$  vs.  $1.43 \pm$   
207  $0.83 \text{ m}^2 \text{ g C}^{-1}$ ) and night ( $2.58 \pm 0.14$  vs.  $1.02 \pm 0.49 \text{ m}^2 \text{ g C}^{-1}$ ), respectively, which is opposed



208 to the results of previous studies. For example, the MAE<sub>365</sub> of WS-BrC are 0.7- and 0.5-fold of  
209 WIS-BrC in winter of Beijing ( $1.22 \pm 0.11$  vs.  $1.66 \pm 0.48 \text{ m}^2 \text{ g C}^{-1}$ ) (Chen and Bond, 2010)  
210 and Xi'an ( $1.00 \pm 0.18$  vs.  $1.82 \pm 1.06 \text{ m}^2 \text{ g C}^{-1}$ ) (Li et al., 2020), respectively. This result  
211 indicates that the chemical composition of BrC in the most polluted city, Shijiazhuang, is  
212 different from other urban areas on primary sources and secondary aging process. However,  
213 both WS-BrC and WIS-BrC have higher MAE<sub>365</sub> and average AAE values during the day than  
214 the night. This suggests that the day-night differences of AAE and MAE<sub>365</sub> of BrC fractions are  
215 likely associated with the different primary emissions and atmospheric aging processes (Cheng  
216 et al., 2016; Wang et al., 2019a; Wang et al., 2020). For example, the AAE and MAE<sub>365</sub> of BrC  
217 emitted from biomass burning (AAE  $\sim 7.31$ , and MAE<sub>365</sub>  $\sim 1.01 \text{ m}^2 \text{ g C}^{-1}$ , respectively) (Siemens  
218 et al., 2022) showed large differences with that from vehicle emissions (AAE  $\sim 10.5$ , and  
219 MAE<sub>365</sub>  $\sim 0.32 \text{ m}^2 \text{ g C}^{-1}$ ) (Xue et al., 2018). Besides, photochemical oxidation of fresh BrC from  
220 coal combustion resulted in considerable changes in AAE and MAE<sub>365</sub>, e.g., the AAE and  
221 MAE<sub>365</sub> of fresh coal combustion emission are 7.2 and  $0.84 \pm 0.54 \text{ m}^2 \text{ g C}^{-1}$ , much higher than  
222 those in aged samples ( $6.4$  and  $0.14 \pm 0.08 \text{ m}^2 \text{ g C}^{-1}$ , respectively) (Ni et al., 2021).

223 Figure 1 (b) shows the light absorption contributions of WS-BrC and WIS-BrC to total  
224 BrC over the wavelength range of 300–500 nm. It is obvious that the absorption contribution  
225 of WS-BrC is increased from 53.8% at 300 nm to 87.4% at 500 nm during the day, and from  
226 38.4% to 61.5% during the night. The higher absorption contributions of WS-BrC at longer  
227 wavelengths during the day compared to that of the night may be related to photo-oxidation  
228 reaction in day time (Wang et al., 2019b; Chen et al., 2021). The absorption contribution of  
229 WS-BrC accounts for  $62 \pm 8\%$  to total BrC absorption at 365 nm during the day, but only  $47 \pm$   
230  $8\%$  during the night. The large difference in BrC light absorption between samples from the  
231 day and those from the night observed in this study is comparable with previous studies (Shen  
232 et al., 2019; Li et al., 2020), and indicates the significant day-night difference in chemical  
233 composition.

### 234 **3.2 Composition and absorption contribution of BrC during day and night.**

235 In total, 38 major chromophores were quantified in WS-BrC and WIS-BrC with HPLC-  
236 PDA-HRMS analysis, and the concentrations of these chromophores are shown in Table S3.

237 According to the characteristics of the molecular structures and absorption spectra, these  
238 chromophores are divided into ten subgroups, including two quinolines, four nitrocatechols, six  
239 nitrophenols, four aromatic alcohols/acids, four 2–3-ring OPAHs, three 4-ring OPAHs, two 3-  
240 ring PAHs, four 4-ring PAHs, five 5-ring PAHs, and four 6-ring PAHs. Detailed information  
241 about these chromophores is listed in Table S4. Figure 2 shows the chemical composition of the  
242 identified BrC components during the day and night. The total concentration of these  
243 chromophores during the day (169.8 ng/m<sup>3</sup>) is similar to that at night (171.8 ng/m<sup>3</sup>), and the  
244 chemical composition of the BrC subgroups is clearly different between the day and night. For  
245 example, nitrocatechols, aromatic alcohols/acids and 2–3-rings OPAHs are the major  
246 contributors to the total mass concentration of identified BrC chromophores during the day  
247 (accounting for 23.3%, 22.3%, and 16.6%, respectively). These BrC chromophores, however,  
248 are the minor components during the night (accounting for 12.1% and 15.6%, and 6.9%,  
249 respectively). This result indicates the enhanced formation of these chromophores during the  
250 day. On the contrary, the relative contributions of nitrophenols and 4–6-ring PAHs are much  
251 lower during the day (15.3% and 15.2%, respectively) than those during the night (35.8% and  
252 24.0%, respectively). During the night, 4-nitrophenol (4NP) contributes 24.4% of the total  
253 concentration, followed by 2-methyl-4-nitrophenol, fluoranthene, and chrysene (2M4NP 4.7%,  
254 FLU 4.6%, CHR 4.6%, respectively). The higher contributions of nitrophenols and 4–6-rings  
255 PAHs at night are likely caused by enhanced primary emissions (Lin et al., 2020; Chen et al.,  
256 2021). Our previous study has found that the emitted organic aerosols from coal combustion  
257 had a clearly increase at midnight in Shijiazhuang (Huang et al., 2019; Lin et al., 2020). Thus,  
258 the large contribute of nitrophenols and 4–6-rings PAHs to total mass concentration at night  
259 that may be impacted by emissions from the coal combustion.

260 To investigate the source of the BrC chromophores, the mass concentrations (these  
261 concentrations of chromophores are OC normalized) of the day and night were compared. The  
262 day-to-night ratios of identified BrC compounds in mass concentrations is shown in Figure 3.  
263 It can be seen that the average day-to-night ratios of WS-BrC chromophores are 4.87 for  
264 quinolines, 3.49 for 2–3-ring OPAHs, 3.47 for nitrocatechols, 0.48 for nitrophenols, and 2.53  
265 for aromatic alcohols/acids, respectively. Previous studies have found that quinolines are

266 important products of fossil fuel combustion, and were used as tracers of the vehicular exhaust  
267 (Banerjee and Zare, 2015; Xue et al., 2018; Lyu et al., 2019). Thus, the higher day-to-night ratio  
268 of quinolines may be due to increased primary emissions from vehicles during the day. Nitro-  
269 phenols and vanillin are typical biomass burning tracers for atmospheric aerosols (Harrison et  
270 al., 2005; Scaramboni et al., 2015; Huang et al., 2021). Previous studies have identified  
271 secondary formation as an important source of phthalic acid (PA) and methyl-nitrocatechols  
272 (Chow et al., 2015; Zhang and Hatakeyama, 2016; Liu et al., 2017). In this study, vanillin,  
273 phthalic acid, and three methyl-nitrocatechols (including 4M5NC, 3M6NC, and 3M5NC)  
274 isomers have high day-to-night ratios (4.16, 3.75 and 3.28, respectively). The high day-to-night  
275 ratios of these BrC chromophores suggest that biomass burning and secondary formation likely  
276 play important roles in the daytime source of BrC.

277 The average day-to-night ratio (~0.48) of nitrophenols is smaller than one, and this result  
278 is similar to previous studies (Yuan et al., 2016; Schnitzler and Abbatt, 2018). Although both  
279 nitrophenols and nitrocatechols can be emitted from biomass burning, they show largely  
280 different day-night variation patterns. The higher concentrations of nitrocatechols during  
281 daytime indicate enhanced secondary formation, which is similar to the results observed in  
282 urban Beijing (Cheng et al., 2021). In addition, previous studies found that emissions from  
283 residential coal-fired heating are significant sources of nitrophenols (Wang et al., 2018; Lu et  
284 al., 2019). The higher concentrations of nitrophenols during nighttime, however, suggest that  
285 they are mainly emitted from primary emission sources such as residential heating during winter  
286 in North China. Compared with the WS-BrC chromophores (the day-to-night ratio > 2.53), the  
287 day-to-night ratios of the WIS-BrC chromophores approach or below one, with average ratios  
288 of 1.46 for 3-ring PAHs, 1.34 for 4-ring OPAHs, 0.74 for 4-ring PAHs, 0.91 for 5-ring PAHs,  
289 and 0.79 for 6-ring PAHs, respectively. A number of studies showed that coal combustion was  
290 the dominant source of PAHs (Wang et al., 2018; Xie et al., 2019; Yuan et al., 2020). Thus, the  
291 local emissions may be responsible for the majority of 4–6-rings PAHs during the night.

292 Figure S2 shows the light absorption contributions of the BrC subgroups to total BrC  
293 subgroups in the wavelength range between 300 and 420 nm (the absorptions above 420 nm  
294 are too low to exactly estimate the contributions), exhibiting large day-night difference. For

295 example, quinolines show evident absorption below 340 nm (3.6% at 310 nm during the day),  
296 but negligible contribution above 360 nm. Nitrophenols exhibit a maximum contribution at  
297 about 350 nm, while nitrocatechols show higher absorption in the wavelength range from 360  
298 to 400 nm. For PAHs, the absorption maxima shift to a longer wavelength with the increase of  
299 the aromatic rings (e.g., 320 nm for 4-ring PAHs and 400 nm for 6-ring PAHs). Overall, the  
300 combined light absorption contributions of nitrophenols, nitrocatechols, and PAHs are 86.5%  
301 and 80.1% (averaged between 300 and 420 nm) at night and day, respectively. This result is  
302 similar to previous studies, in which PAHs and nitro aromatic compounds were identified as  
303 the major chromophores (Huang et al., 2020; Yuan et al., 2020).

304 The light absorption contribution of these BrC subgroups exhibits obvious day-night  
305 differences. For example, the absorption contribution of 2–3-rings OPAHs and nitrocatechols  
306 at 365 nm increased by ~2.0 and ~3.5 times during the day compared to that during the night  
307 (see Figure S3). This result differs from previous studies (Kampf et al., 2012; Gao et al., 2022),  
308 which indicated that light absorption of BrC compounds were enhanced after exposure to photo-  
309 oxidation. On the other hand, the absorption contributions of nitrophenols and 4–6-rings PAHs  
310 at 365 nm are ~1.6 times and ~2.2 times higher at night than at day, respectively. The day-night  
311 difference of light absorption of nitrophenols is comparable with previous studies (Harrison et  
312 al., 2005; Wang et al., 2020). High absorbance of nitrophenols at night is closely related to their  
313 higher mass fraction at night. The absorption characteristics of 4–6-ring PAHs are significantly  
314 different from the nitro-phenols, and their absorption per unit mass is larger than that of nitro-  
315 phenols. The per unit mass absorbance of PAHs much higher than the low-ring aromatic  
316 hydrocarbons (e.g., aromatic alcohols/acids) are due to their strongly conjugated systems. It is  
317 worth noting that the absorption contributions of some BrC compounds (including quinolines,  
318 aromatic alcohols/acids, 4-ring OPAHs, 3-ring PAHs four subgroups) are much lower than  
319 those of the above-mentioned BrC compounds because of their lower mass concentration or  
320 light absorption coefficient.

### 321 **3.3 Comparisons between the low and high pollution period.**

322 The relative contributions of day-night subgroups of BrC chromophores in light absorption  
323 and mass concentration were further investigated for different pollution levels. The sampling

324 campaign was classified into low-pollution period ( $PM_{2.5} < 150 \mu\text{g m}^{-3}$ ) and high-pollution  
325 period ( $PM_{2.5} > 250 \mu\text{g m}^{-3}$ ). Figure 4 (a) shows the mass fractional contributions of the  
326 identified subgroups during these periods, which show an evidently different during the day  
327 and night. For example, the mass fraction of quinolines during the day ( $\sim 24.1\%$ ) is much higher  
328 than during the night (3.4%) at low-pollution period, which may be related to increased vehicle  
329 emissions at day (Rogge et al., 1993; Lyu et al., 2019). Moreover, during the low-pollution  
330 period, with good atmospheric dispersion conditions during the day, the fractional concentration  
331 of BrC is only  $56.9 \text{ ng m}^{-3}$  much lower than the nights and high-pollution periods. In the high-  
332 pollution period, however, the mass concentration of quinolines is much lower than other BrC  
333 chromophores and there is no evident difference between day and night. The mass fraction of  
334 aromatic alcohols/acids during the day (35.4%) is much higher than during the night (12.0%)  
335 at low-pollution period. For high-pollution period, the mass fraction of aromatic alcohols/acids  
336 shows little difference between the day and night. However, their mass concentration during  
337 the day ( $55.5 \text{ ng m}^{-3}$ ) is higher than that during the night ( $31.9 \text{ ng m}^{-3}$ ). Thereinto, the mass  
338 concentration of phthalic acid (a tracer from photochemical oxidation) contributes more than  
339 60% to the aromatic alcohols/acids at day for low and high-pollution period (Zhang and  
340 Hatakeyama, 2016). This evidence may be suggesting that there is stronger photo-chemical  
341 oxidation for aromatic alcohols/acids during the day, especially at low-pollution period.

342 The mass fractional contribution of nitrocatechols is lower during the day than the night  
343 at low-pollution period, while there is obvious secondary formation during the day for high-  
344 pollution period. This likely suggests that the daytime conditions of the high-pollution period  
345 are conducive for the generation of nitrocatechols. The mass fractional contribution of PAHs  
346 during the day is much lower than the night at low-pollution period. At night, residential coal  
347 heating is an important source of PAHs, and therefore the daytime contributions of PAHs are  
348 much lower than nighttime (Wang et al., 2017; Ni et al., 2021). While there is no day-night  
349 difference for PAHs at high-pollution period, which is related to the stable sources and stagnant  
350 weather conditions (Huang et al., 2019; Lin et al., 2020). It is noteworthy that the mass  
351 contributions of the nitrophenols (nighttime is 2–3 times more than daytime) and 2–3-rings  
352 OPAHs (daytime is  $\sim 2$  times more than nighttime) is opposite between the day and night. This

353 demonstrates that they have stable sources compared to other BrC subgroups even during the  
354 low-pollution period and high-pollution period. The higher mass fractional contribution of 2–  
355 3-rings OPAHs during the day is related to photochemical oxidation. Nitrophenols exhibit a  
356 higher mass fractional contribution during the night than the day, indicating a significant  
357 contribution from primary emissions (Lu et al., 2019; Lin et al., 2020). Besides, previous  
358 investigations have shown that NO<sub>x</sub> concentrations and relative humidity are higher at night in  
359 Shijiazhuang, which may have accelerated the formation of nitrophenols in the dark (Yuan et  
360 al., 2016; Huang et al., 2019). This result exhibits a clear day-night difference during the low-  
361 pollution period than high-pollution period, which indicates that the low-pollution period is  
362 easily influenced by the external environment (e.g., solar radiation and wind speed).

363 The day-night light absorption contribution of WS-BrC and WIS-BrC chromophores in  
364 different pollution periods is shown in Figure 4 (b). For the low-pollution period, the light  
365 absorption contribution of the ten BrC subgroups shows a large difference during the day and  
366 night. Thereinto, the WS-BrC chromophores (e.g., quinolines, nitrophenols and nitrocatechols)  
367 is the main contributor (accounting for ~75% at 365 nm) of total identified BrC during the day.  
368 While, the WIS-BrC chromophores (e.g., 4–6-rings PAHs) become an abundance contributor  
369 (accounting for ~65% at 365 nm) during the night. There is an obvious day-night differences in  
370 light absorption at low-pollution period, which is consistent with the difference in their mass  
371 concentration contribution. Different from the low-pollution period, the light absorption  
372 contribution of the total WS-BrC and WIS-BrC chromophores showed no significant day-night  
373 differences during the high-pollution period. However, the absorption contributions of  
374 subgroups in WS-BrC chromophores have a significant day-night difference (e.g., nitrocatechol  
375 and nitrophenols) during the high-pollution period, which is due to the change of the mass  
376 contributions. WS-BrC chromophores have stronger light absorption both during the day and  
377 night compared to the WIS-BrC chromophores at high pollution period. Specifically, the  
378 absorption contribution of nitrocatechols and nitrophenols combined accounts for 66.1% at day  
379 and 60.7% at night at 365 nm, respectively, which depend on the different emission sources or  
380 formation mechanisms between during the day and night. Our results show a significant day-  
381 night differences in mass contributions and absorption contributions of BrC components at

382 different pollution levels. This suggests that the variation of BrC chromophores in different  
383 pollution periods may be caused by different sources and weather conditions.

#### 384 **4 Conclusions**

385 In general, our study shows the large day-night differences in optical properties and  
386 chemical composition of the bulk BrC in urban atmosphere. Thereinto, WS-BrC is the main  
387 light-absorbing contributors during the day, while WIS-BrC is main light-absorbing compound  
388 at night. The polar WS-BrC has higher MAE<sub>365</sub> compared to the less-polar WIS-BrC, mainly  
389 due to the different conjugate systems and functional groups in the two fractions. Different  
390 types of the identified BrC chromophores exhibit unique characteristics of day-night differences,  
391 reflecting their particular sources and formation pathways. For example, nitrocatechols and 2–  
392 3-rings OPAHs are important contributors to mass concentration and light absorption during  
393 the day, while 4–6-rings PAHs and nitrophenols become the significant contributors at night.

394 Day-night differences of BrC chromophores are associated with different sources during  
395 day (mainly secondary formation and vehicle emission) and night (mainly emissions from  
396 residential heating) as well as the dynamic development of planetary boundary layer height.  
397 Moreover, these day-night differences are largely affected by the air pollution level, which  
398 determines the concentrations of BrC precursors (e.g., aromatic hydrocarbon and phenols) and  
399 oxidants (e.g., NO<sub>x</sub>, NO<sub>3</sub><sup>·</sup> and OH), as well as meteorological conditions (e.g., solar irradiation  
400 and RH) (Liu et al., 2012; Laskin et al., 2015; Wang et al., 2019). For example, our results found  
401 that the day-night difference of BrC fractions is more pronounced in chemical composition and  
402 light absorption during the low-pollution period than high-pollution period. These factors may  
403 show different effects on the formation and photobleaching of different types of the identified  
404 chromophores. However, our current understanding of the formation mechanisms of and  
405 influencing factors on these identified chromophores is still incomplete (Huang et al., 2018;  
406 Yuan et al., 2020). Therefore, a combination of more laboratory and field studies is needed to  
407 (1) make comprehensive characterization of the chromophore composition BrC in ambient  
408 aerosol; (2) explore thoroughly the formation mechanisms of different types of BrC  
409 chromophore. This will significantly enhance our understanding of atmospheric BrC formation  
410 mechanisms and therefore improve the accuracy of the atmospheric effects of BrC in air quality

411 and climate models.



412 **Data availability.** Detailed data can be obtained from <https://doi.org/10.5281/zenodo.7690230>.

413 **Author contributions.** Ru-jin Huang designed the study. Data analysis was done by Yuquan Gong  
414 and Rujin Huang. Yuquan Gong and Rujin Huang interpreted data, prepared the display items and  
415 wrote the manuscript. Lu Yang, Ting Wang, Wei Yuan, Wei Xu, Wenjuan Cao, Yang Wang, and  
416 Yongjie Li commented on and discussed the manuscript.

417 **Competing interests.** The authors declare that they have no conflict of interest.

418 **Acknowledgements.** We are very grateful to the National Natural Science Foundation of China  
419 (NSFC) (No. 41925015), the Strategic Priority Research Program of Chinese Academy of  
420 Sciences (No. XDB40000000), the Chinese Academy of Sciences (No. ZDBS-LY-DQC001),  
421 and the Cross Innovative Team fund from the State Key Laboratory of Loess and Quaternary  
422 Geology (No. SKLLQGTD1801) supported this study.

423 **Financial support.** This work was supported by the National Natural Science Foundation of  
424 China (NSFC) under Grant No. 41925015, the Strategic Priority Research Program of Chinese  
425 Academy of Sciences (No. XDB40000000), the Chinese Academy of Sciences (No. ZDBS-LY-  
426 DQC001), and the Cross Innovative Team fund from the State Key Laboratory of Loess and  
427 Quaternary Geology (No. SKLLQGTD1801).

428 **References**

- 429 Alcanzare, R. J. C.: Polycyclic aromatic compounds in wood soot extracts from Henan, China, 2006.
- 430 Banerjee, S. and Zare, R. N.: Syntheses of isoquinoline and substituted quinolines in charged  
431 microdroplets, *Angew. Chem.*, 127, 15008-15012, 2015.
- 432 Chen, L.-W. A., Chow, J. C., Wang, X., Cao, J., Mao, J., and Watson, J. G.: Brownness of Organic  
433 Aerosol over the United States: Evidence for Seasonal Biomass Burning and Photobleaching  
434 Effects, *Environ. Sci. Technol.*, 55, 8561-8572, 10.1021/acs.est.0c08706, 2021.
- 435 Chen, Y. and Bond, T. C.: Light absorption by organic carbon from wood combustion, *Atmos. Chem.*  
436 *Phys.*, 10, 1773-1787, 10.5194/acp-10-1773-2010, 2010.
- 437 Cheng, Y., He, K.-b., Du, Z.-y., Engling, G., Liu, J.-m., Ma, Y.-l., Zheng, M., and Weber, R. J.: The  
438 characteristics of brown carbon aerosol during winter in Beijing, *Atmos. Environ.*, 127, 355-364,  
439 10.1016/j.atmosenv.2015.12.035, 2016.
- 440 Cheng, X., Chen, Q., Li, Y., Huang, G., Liu, Y., Lu, S., Zheng, Y., Qiu, W., Lu, K., Qiu, X., Bianchi,  
441 F., Yan, C., Yuan, B., Shao, M., Wang, Z., Canagaratna, M. R., Zhu, T., Wu, Y., and Zeng, L.:  
442 Secondary Production of Gaseous Nitrated Phenols in Polluted Urban Environments, *Environ.*  
443 *Sci. Technol.*, 55, 4410-4419, 10.1021/acs.est.0c07988, 2021.
- 444 Chow, J. C., Watson, J. G., Robles, J., Wang, X., Chen, L.-W. A., Trimble, D. L., Kohl, S. D., Tropp,  
445 R. J., and Fung, K. K.: Quality assurance and quality control for thermal/optical analysis of  
446 aerosol samples for organic and elemental carbon, *Anal. Bioanal. Chem.*, 401, 3141-3152, 2011.
- 447 Chow, K. S., Huang, X. H., and Yu, J. Z.: Quantification of nitroaromatic compounds in atmospheric  
448 fine particulate matter in Hong Kong over 3 years: field measurement evidence for secondary  
449 formation derived from biomass burning emissions, *Environ.Chem.*, 13, 665-673, 2015.
- 450 Dat, N. D. and Chang, M. B.: Review on characteristics of PAHs in atmosphere, anthropogenic  
451 sources and control technologies, *Sci Total Environ.*, 609, 682-693,  
452 10.1016/j.scitotenv.2017.07.204, 2017.
- 453 Deng, J., Ma, H., Wang, X., Zhong, S., Zhang, Z., Zhu, J., Fan, Y., Hu, W., Wu, L., Li, X., Ren, L.,  
454 Pavuluri, C. M., Pan, X., Sun, Y., Wang, Z., Kawamura, K., and Fu, P.: Measurement report:  
455 Optical properties and sources of water-soluble brown carbon in Tianjin, North China – insights  
456 from organic molecular compositions, *Atmos. Chem. Phys.*, 22, 6449-6470, 10.5194/acp-22-  
457 6449-2022, 2022.
- 458 Gao, Y., Wang, Q., Li, L., Dai, W., Yu, J., Ding, L., Li, J., Xin, B., Ran, W., and Han, Y.: Optical  
459 properties of mountain primary and secondary brown carbon aerosols in summertime, *Sci Total*  
460 *Environ.*, 806, 150570, 2022.
- 461 Hammer, M. S., Martin, R. V., van Donkelaar, A., Buchard, V., Torres, O., Ridley, D. A., and Spurr,  
462 R. J. D.: Interpreting the ultraviolet aerosol index observed with the OMI satellite instrument to  
463 understand absorption by organic aerosols: implications for atmospheric oxidation and direct  
464 radiative effects, *Atmos. Chem. Phys.*, 16, 2507-2523, 10.5194/acp-16-2507-2016, 2016.
- 465 Harrison, M. A., Barra, S., Borghesi, D., Vione, D., Arsene, C., and Olariu, R. I.: Nitrated phenols  
466 in the atmosphere: a review, *Atmos. Environ.*, 39, 231-248, 2005.
- 467 Hems, R. F. and Abbatt, J. P. D.: Aqueous Phase Photo-oxidation of Brown Carbon Nitrophenols:  
468 Reaction Kinetics, Mechanism, and Evolution of Light Absorption, *ACS Earth Space Chem.*, 2,  
469 225-234, 10.1021/acsearthspacechem.7b00123, 2018.
- 470 Hecobian, A., Zhang, X., Zheng, M., Frank, N., Edgerton, E. S., and Weber, R. J.: Water-Soluble  
471 Organic Aerosol material and the light-absorption characteristics of aqueous extracts measured

472 over the Southeastern United States, *Atmos. Chem. Phys.*, 10, 5965-5977, 2010.

473 Huang, R.-J., Wang, Y., Cao, J., Lin, C., Duan, J., Chen, Q., Li, Y., Gu, Y., Yan, J., and Xu, W.:  
474 Primary emissions versus secondary formation of fine particulate matter in the most polluted city  
475 (Shijiazhuang) in North China, *Atmos. Chem. Phys.*, 19, 2283-2298, 2019.

476 Huang, R.-J., Yang, L., Cao, J., Chen, Y., Chen, Q., Li, Y., Duan, J., Zhu, C., Dai, W., and Wang, K.:  
477 Brown carbon aerosol in urban Xi'an, Northwest China: the composition and light absorption  
478 properties, *Environ. Sci. Technol.*, 52, 6825-6833, 2018.

479 Huang, R.-J., Yang, L., Shen, J., Yuan, W., Gong, Y., Ni, H., Duan, J., Yan, J., Huang, H., and You,  
480 Q.: Chromophoric Fingerprinting of Brown Carbon from Residential Biomass Burning, *Environ.*  
481 *Sci. Technol. Lett.*, 2021.

482 Huang, R.-J., Zhang, Y., Bozzetti, C., Ho, K.-F., Cao, J.-J., Han, Y., Daellenbach, K. R., Slowik, J.  
483 G., Platt, S. M., and Canonaco, F.: High secondary aerosol contribution to particulate pollution  
484 during haze events in China, *Nature*, 514, 218-222, 2014.

485 Huang, R. J., Yang, L., Shen, J., Yuan, W., Gong, Y., Guo, J., Cao, W., Duan, J., Ni, H., Zhu, C., Dai,  
486 W., Li, Y., Chen, Y., Chen, Q., Wu, Y., Zhang, R., Dusek, U., O'Dowd, C., and Hoffmann, T.:  
487 Water-Insoluble Organics Dominate Brown Carbon in Wintertime Urban Aerosol of China:  
488 Chemical Characteristics and Optical Properties, *Environ Sci Technol.*, 54, 7836-7847,  
489 10.1021/acs.est.0c01149, 2020.

490 Iinuma, Y., Böge, O., Gräfe, R., and Herrmann, H.: Methyl-nitrocatechols: atmospheric tracer  
491 compounds for biomass burning secondary organic aerosols, *Environ Sci Technol.*, 44, 8453-  
492 8459, 2010.

493 Kampf, C. J., Jakob, R., and Hoffmann, T.: Identification and characterization of aging products in  
494 the glyoxal/ammonium sulfate system—implications for light-absorbing material in atmospheric  
495 aerosols, *Atmos. Chem. Phys.*, 12, 6323-6333, 2012.

496 Kasthuriarachchi, N. Y., Rivellini, L. H., Chen, X., Li, Y. J., and Lee, A. K. Y.: Effect of Relative  
497 Humidity on Secondary Brown Carbon Formation in Aqueous Droplets, *Environ Sci Technol.*,  
498 54, 13207-13216, 10.1021/acs.est.0c01239, 2020.

499 Kirchstetter, T. W., Novakov, T., and Hobbs, P. V.: Evidence that the spectral dependence of light  
500 absorption by aerosols is affected by organic carbon, *J Geophys Res-Atmos.*, 109, 2004.

501 Kitanovski, Z., Grgić, I., Yasmeen, F., Claeys, M., and Čusak, A.: Development of a liquid  
502 chromatographic method based on ultraviolet–visible and electrospray ionization mass  
503 spectrometric detection for the identification of nitrocatechols and related tracers in biomass  
504 burning atmospheric organic aerosol, *Rapid Commun Mass Sp.*, 26, 793-804, 2012.

505 Laskin, A., Laskin, J., and Nizkorodov, S. A.: Chemistry of atmospheric brown carbon, *Chem Rev.*,  
506 115, 4335-4382, 10.1021/cr5006167, 2015.

507 Li, J., Zhang, Q., Wang, G., Li, J., Wu, C., Liu, L., Wang, J., Jiang, W., Li, L., and Ho, K. F.: Optical  
508 properties and molecular compositions of water-soluble and water-insoluble brown carbon (BrC)  
509 aerosols in northwest China, *Atmos. Chem. Phys.*, 20, 4889-4904, 2020.

510 Li, X., Zhao, Q., Yang, Y., Zhao, Z., Liu, Z., Wen, T., Hu, B., Wang, Y., Wang, L., and Wang, G.:  
511 Composition and sources of brown carbon aerosols in megacity Beijing during the winter of 2016,  
512 *Atmos. Res.*, 262, 105773, 2021.

513 Lin, C., Huang, R.-J., Xu, W., Duan, J., Zheng, Y., Chen, Q., Hu, W., Li, Y., Ni, H., and Wu, Y.:  
514 Comprehensive Source Apportionment of Submicron Aerosol in Shijiazhuang, China: Secondary  
515 Aerosol Formation and Holiday Effects, *ACS Earth and Space Chem.*, 4, 947-957, 2020.

516 Lin, P., Bluvshstein, N., Rudich, Y., Nizkorodov, S. A., Laskin, J., and Laskin, A.: Molecular  
517 Chemistry of Atmospheric Brown Carbon Inferred from a Nationwide Biomass Burning Event,  
518 *Environ. Sci. Technol.*, 51, 11561-11570, 10.1021/acs.est.7b02276, 2017.

519 Lin, P., Rincon, A. G., Kalberer, M., and Yu, J. Z.: Elemental Composition of HULIS in the Pearl  
520 River Delta Region, China: Results Inferred from Positive and Negative Electrospray High  
521 Resolution Mass Spectrometric Data, *Environ. Sci. Technol.*, 46, 7454-7462, 2012.

522 Liu, S., Shilling, J. E., Song, C., Hiranuma, N., Zaveri, R. A., and Russell, L. M.: Hydrolysis of  
523 organonitrate functional groups in aerosol particles, *Aerosol. Sci. Technol.*, 46, 1359-1369, 2012.

524 Liu, J., Lin, P., Laskin, A., Laskin, J., Kathmann, S. M., Wise, M., Caylor, R., Imholt, F., Selimovic,  
525 V., and Shilling, J. E.: Optical properties and aging of light-absorbing secondary organic aerosol,  
526 *Atmos. Chem. Phys.*, 16, 12815-12827, 10.5194/acp-16-12815-2016, 2016.

527 Liu, W.-J., Li, W.-W., Jiang, H., and Yu, H.-Q.: Fates of chemical elements in biomass during its  
528 pyrolysis, *Chem. Rev.*, 117, 6367-6398, 2017.

529 Lu, C., Wang, X., Li, R., Gu, R., Zhang, Y., Li, W., Gao, R., Chen, B., Xue, L., and Wang, W.:  
530 Emissions of fine particulate nitrated phenols from residential coal combustion in China, *Atmos.*  
531 *Environ.*, 203, 10-17, <https://doi.org/10.1016/j.atmosenv.2019.01.047>, 2019.

532 Lyu, R., Shi, Z., Alam, M. S., Wu, X., Liu, D., Vu, T. V., Stark, C., Fu, P., Feng, Y., and Harrison, R.  
533 M.: Insight into the composition of organic compounds ( $\geq C_6$ ) in PM 2.5 in wintertime in Beijing,  
534 China, *Atmos. Chem. Phys.*, 19, 10865-10881, 2019.

535 Ni, H., Huang, R.-J., Pieber, S. M., Corbin, J. C., Stefenelli, G., Pospisilova, V., Klein, F., Gysel-  
536 Beer, M., Yang, L., and Baltensperger, U.: Brown carbon in primary and aged coal combustion  
537 emission, *Environ. Sci. Technol.*, 55, 5701-5710, 2021.

538 Rogge, W. F., Hildemann, L. M., Mazurek, M. A., Cass, G. R., and Simoneit, B. R.: Sources of fine  
539 organic aerosol. 2. Noncatalyst and catalyst-equipped automobiles and heavy-duty diesel trucks,  
540 *Environ. Sci. Technol.*, 27, 636-651, 1993.

541 Scaramboni, C., Urban, R. C., Lima-Souza, M., Nogueira, R. F. P., Cardoso, A. A., Allen, A. G., and  
542 Campos, M. d. M.: Total sugars in atmospheric aerosols: An alternative tracer for biomass burning,  
543 *Atmos. Environ.*, 100, 185-192, 2015.

544 Schnitzler, E. G. and Abbatt, J. P.: Heterogeneous OH oxidation of secondary brown carbon aerosol,  
545 *Atmos. Chem. Phys.*, 18, 14539-14553, 2018.

546 Shen, R., Liu, Z., Chen, X., Wang, Y., Wang, L., Liu, Y., and Li, X.: Atmospheric levels, variations,  
547 sources and health risk of PM<sub>2.5</sub>-bound polycyclic aromatic hydrocarbons during winter over  
548 the North China Plain, *Sci. Total Environ.*, 655, 581-590, 2019.

549 Siemens, K., Morales, A., He, Q., Li, C., Hettiyadura, A. P., Rudich, Y., and Laskin, A.: Molecular  
550 Analysis of Secondary Brown Carbon Produced from the Photooxidation of Naphthalene,  
551 *Environ. Sci. Technol.*, 56, 3340-3353, 2022.

552 Teich, M., van Pinxteren, D., Wang, M., Kecorius, S., Wang, Z., Müller, T., Močnik, G., and  
553 Herrmann, H.: Contributions of nitrated aromatic compounds to the light absorption of water-  
554 soluble and particulate brown carbon in different atmospheric environments in Germany and  
555 China, *Atmos. Chem. Phys.*, 17, 1653-1672, 2017.

556 Wang, H., Gao, Y., Wang, S., Wu, X., Liu, Y., Li, X., Huang, D., Lou, S., Wu, Z., and Guo, S.:  
557 Atmospheric processing of nitrophenols and nitrocresols from biomass burning emissions, *J.*  
558 *Geophys. Res. Atmos.*, 125, e2020JD033401, 2020.

559 Wang, L., Wang, X., Gu, R., Wang, H., Yao, L., Wen, L., Zhu, F., Wang, W., Xue, L., Yang, L., Lu,

560 K., Chen, J., Wang, T., Zhang, Y., and Wang, W.: Observations of fine particulate nitrated phenols  
561 in four sites in northern China: concentrations, source apportionment, and secondary formation,  
562 *Atmos. Chem. Phys.*, 18, 4349-4359, 10.5194/acp-18-4349-2018, 2018.

563 Wang, Q., Han, Y., Ye, J., Liu, S., Pongpiachan, S., Zhang, N., Han, Y., Tian, J., Wu, C., and Long,  
564 X.: High contribution of secondary brown carbon to aerosol light absorption in the southeastern  
565 margin of Tibetan Plateau, *Geophys.Res. Lett.*, 46, 4962-4970, 2019a.

566 Wang, X., Gu, R., Wang, L., Xu, W., Zhang, Y., Chen, B., Li, W., Xue, L., Chen, J., and Wang, W.:  
567 Emissions of fine particulate nitrated phenols from the burning of five common types of biomass,  
568 *Environ Pollut.*, 230, 405-412, 10.1016/j.envpol.2017.06.072, 2017.

569 Wang, Y., Hu, M., Wang, Y., Zheng, J., Shang, D., Yang, Y., Liu, Y., Li, X., Tang, R., and Zhu, W.:  
570 The formation of nitro-aromatic compounds under high NO<sub>x</sub> and anthropogenic VOC conditions  
571 in urban Beijing, China, *Atmos. Chem. Phys.*, 19, 7649-7665, 2019b.

572 Xie, C., Xu, W., Wang, J., Wang, Q., Liu, D., Tang, G., Chen, P., Du, W., Zhao, J., and Zhang, Y.:  
573 Vertical characterization of aerosol optical properties and brown carbon in winter in urban Beijing,  
574 China, *Atmos. Chem. Phys.*, 19, 165-179, 2019.

575 Xue, X., Zeng, M., and Wang, Y.: Highly active and recyclable Pt nanocatalyst for hydrogenation  
576 of quinolines and isoquinolines, *Applied Catalysis A: General.*, 560, 37-41, 2018.

577 Yuan, B., Liggio, J., Wentzell, J., Li, S.-M., Stark, H., Roberts, J. M., Gilman, J., Lerner, B., Warneke,  
578 C., and Li, R.: Secondary formation of nitrated phenols: insights from observations during the  
579 Uintah Basin Winter Ozone Study (UBWOS) 2014, *Atmos. Chem. Phys.*, 16, 2139-2153, 2016.

580 Yuan, W., Huang, R.-J., Yang, L., Guo, J., Chen, Z., Duan, J., Wang, T., Ni, H., Han, Y., and Li, Y.:  
581 Characterization of the light-absorbing properties, chromophore composition and sources of  
582 brown carbon aerosol in Xi'an, northwestern China, *Atmos. Chem. Phys.*, 20, 5129-5144, 2020.

583 Yuan, W., Huang, R.-J., Yang, L., Wang, T., Duan, J., Guo, J., Ni, H., Chen, Y., Chen, Q., and Li, Y.:  
584 Measurement report: PM<sub>2.5</sub>-bound nitrated aromatic compounds in Xi'an, Northwest China—  
585 seasonal variations and contributions to optical properties of brown carbon, *Atmos. Chem. Phys.*,  
586 21, 3685-3697, 2021.

587 Zhan, Y., Li, J., Tsona, N. T., Chen, B., Yan, C., George, C., and Du, L.: Seasonal variation of water-  
588 soluble brown carbon in Qingdao, China: Impacts from marine and terrestrial emissions, *Environ.*  
589 *Res.*, 212, 113144, <https://doi.org/10.1016/j.envres.2022.113144>, 2022.

590 Zhang, S., Zhang, W., Wang, K., Shen, Y., Hu, L., and Wang, X.: Concentration, distribution and  
591 source apportionment of atmospheric polycyclic aromatic hydrocarbons in the southeast suburb  
592 of Beijing, China, *Environ. Monit. Assess.*, 151, 197-207, 2009.

593 Zhang, Y. and Hatakeyama, S.: New directions: Need for better understanding of source and  
594 formation process of phthalic acid in aerosols as inferred from, *Atmos. Environ.*, 140, 147e149,  
595 2016.

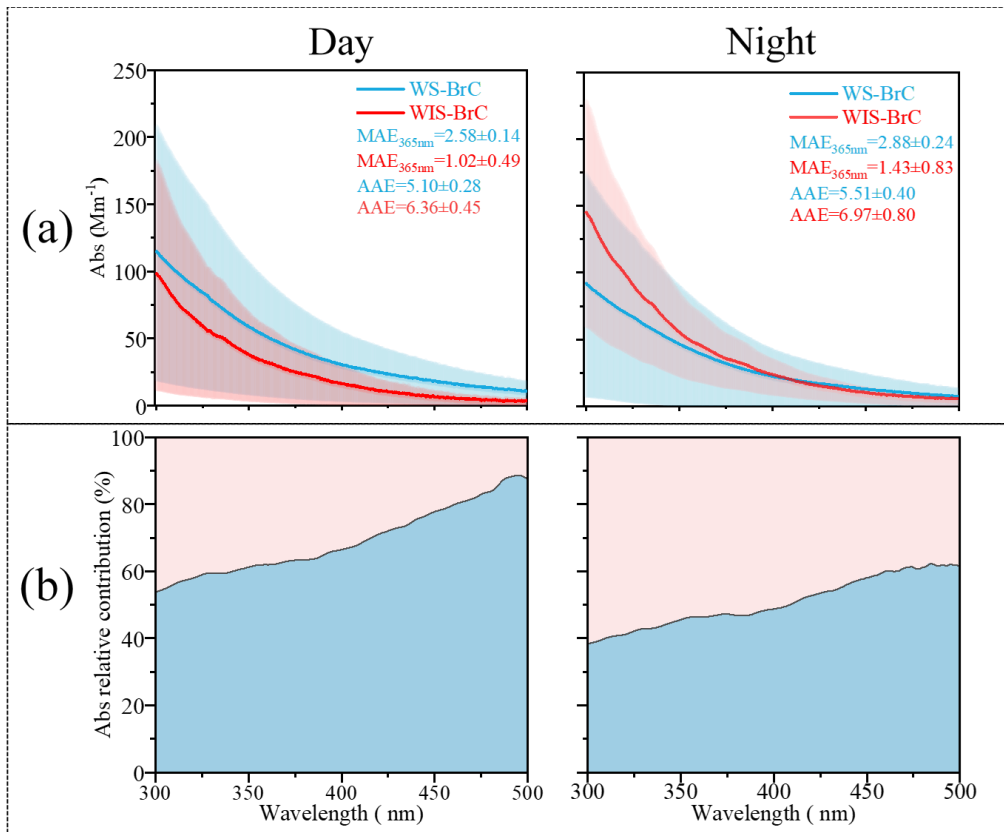


**Figure 1.** (a) Day-night absorption spectra (Abs, in the wavelength range of 300–500 nm), mass absorption efficiency (MAE, determined at 365 nm), and absorption Ångström exponent (AAE, calculated between 300 and 400 nm) of water-soluble/insoluble BrC (WS-/WIS-BrC) in Shijiazhuang. (b) Light-absorbing proportion of WS-BrC and WIS-BrC between 300 to 500 nm.

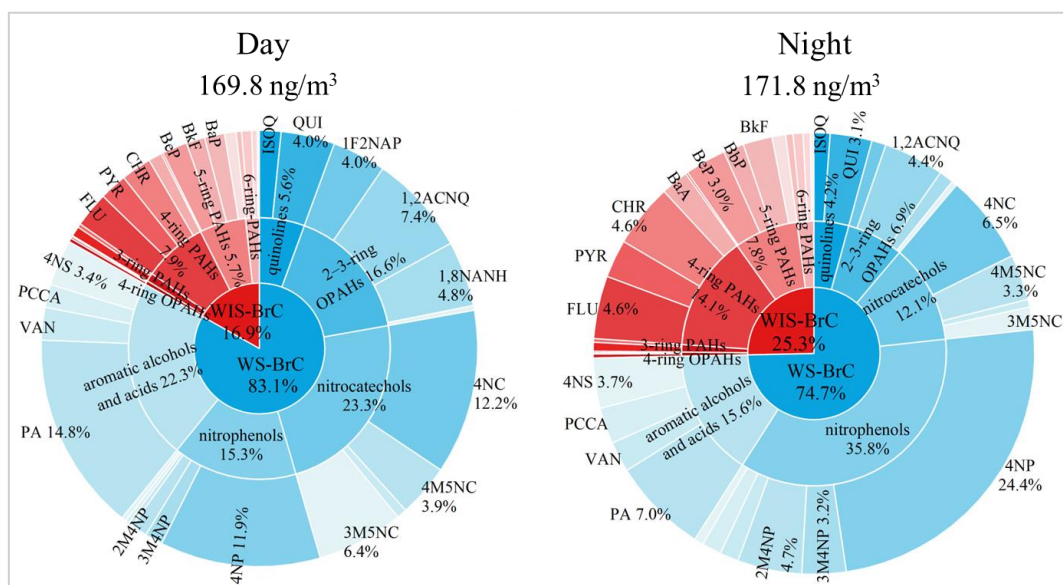


**Figure 2.** Mass fraction of the identified BrC chromophores during the day and night (details

of the identified BrC chromophores are shown in Table S1).

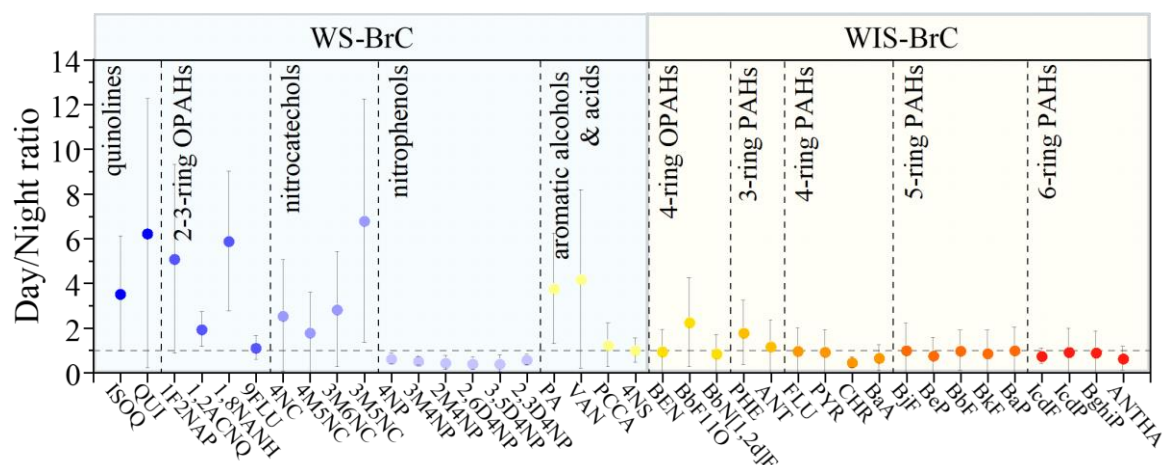


**Figure 3.** Day-to-night ratios of the concentrations of different BrC chromophores.

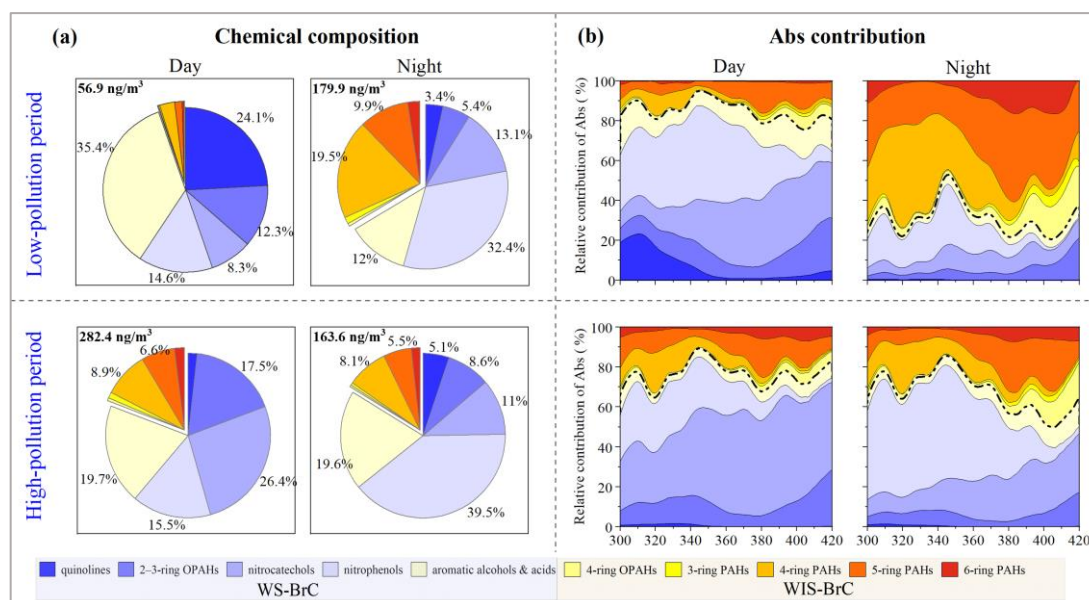


**Figure 4.** Day-night fractional contributions of mass concentrations (a) and light absorption (b) of the ten BrC subgroups in low-pollution period and high-pollution period. Here the BrC chromophore is the main chromophore substance that has been identified. In (b) WS-BrC is below the dotted line and WIS-BrC is above the dotted line.